UNIVERSITÀ DEGLI STUDI DI PALERMO

Dottorato di Ricerca in Medicina Sperimentale e Molecolare
Referente: Prof. Francesco Cappello
Dipartimento di Biomedicina Sperimentale e Neuroscienze Cliniche

Role of adrenomedullin

in the acute respiratory distress syndrome

Tesi di dottorato di:
Claudia Mosca

Tutor:
***Chiar.mo Prof*. Sabrina David**
SSD: BIO/16

Co-Tutor:
Chiar.mo Prof. Giovanni Li Volti
SSD: BIO/10

TRIENNIO 2013-2015

INDEX

1. Respiratory distress syndromes **4**

1.1. Definition **4**

1.2. Epidemology and pathogenesis of ARDS **5**

2. Adrenomedullin **9**

2.1 Discovery and biochemistry **9**

2.2 Molecular Characterization of AM Receptor **12**

3. Aim of the study **15**

4. Materials and Methods **16**

4.1 Cell culture and pharmacological treatments 16

4.2 Cell viability evaluation cytofluorimetric analysis 16

4.3 Annexin V and dead cell evaluation by cytofluorimetric analysis 16

4.4 Reactive Oxygen Species evaluation by cytofluorimetric analysis 17

4.5 Glutathione measurement 17

4.6 ERK1/2 phosphoylation assessment by in-cell western 17

4.7 RNA extraction and qRT-PCR 18

4.8 Animals 19

4.9 Experimental groups 19

4.10 Induction of lung injury by LPS 20

4.11 Measurement of fluid content in lung 20

4.12 Histological examination 20

4.13 Citokynes Proteome Profiler Array 20

4.14 Statistical Analysis 22

5. Results **22**

5.1 Cell Viability 22

5.2 Apoptosis evaluation by cytofluorimetric Annexin V expression 22

5.3 Reactive Oxygen Species formation 23

5.4 Reduced glutathione content measurement 23

5.5 ERK1/2 phosphorylation assessment by in-cell western 24

5.6 Inflammatory mediators gene expression 25

5.7 Effects of AM on LPS-induced lung injury and fluid content 26

5.8 Citokynes Proteome Profiler Array 27

6. Discussion 28

7. Acknowledgment 30

8. References 31

CHAPTER I

RESPIRATORY DISTRESS SYNDROMES

1.1 Definition

Respiratory distress syndromes consist of two major diseases both associated with lung failure. These include two forms identified as IRDS and ARDS. IRDS shape (or infant respiratory distress syndrome) is a congenital disorder that is highly frequent in preterm birth cases. In fact, lung has not yet acquired the ability to synthesize apoproteins of surfactant thus leading to both inflammatory and apoptotic phenomenon involving oxidative lung parenchyma and damage the alveolar epithelium and vessel growth. Acute respiratory distress syndrome (ARDS) is a life-threatening pulmonary syndrome characterized by the acute growth of diffuse lung injury in the setting of a known insult such trauma, sepsis, pneumonia, transfusion, or aspiration (Figure 1). The clinical features of ARDS are hypoxemic respiratory failure requiring positive pressure ventilation and acute diffuse bilateral lung infiltrates on chest radiography (Figure 2). The diagnostic criteria for ARDS have evolved since the syndrome was first recognized in 1967 (Ashbaugh et al., 1967) and were most recently updated in the 2012 Berlin Definition of ARDS.

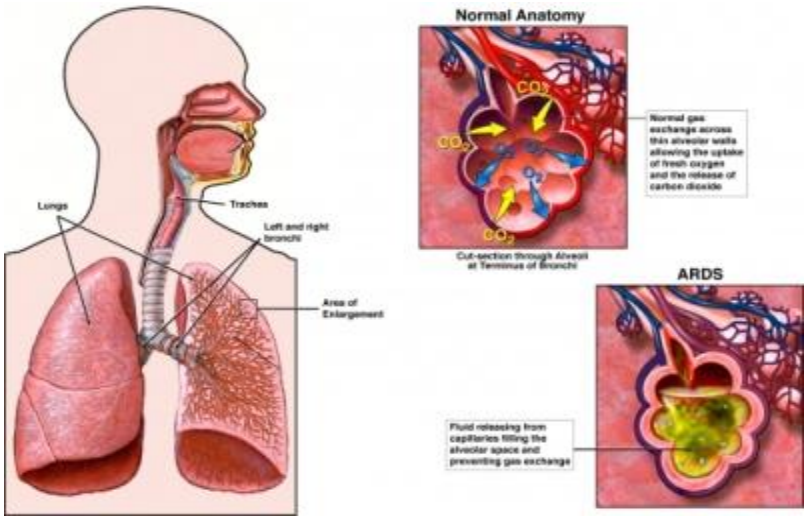

Figure 1. Normal anatomy of the lung compared to ARDS.

A

B

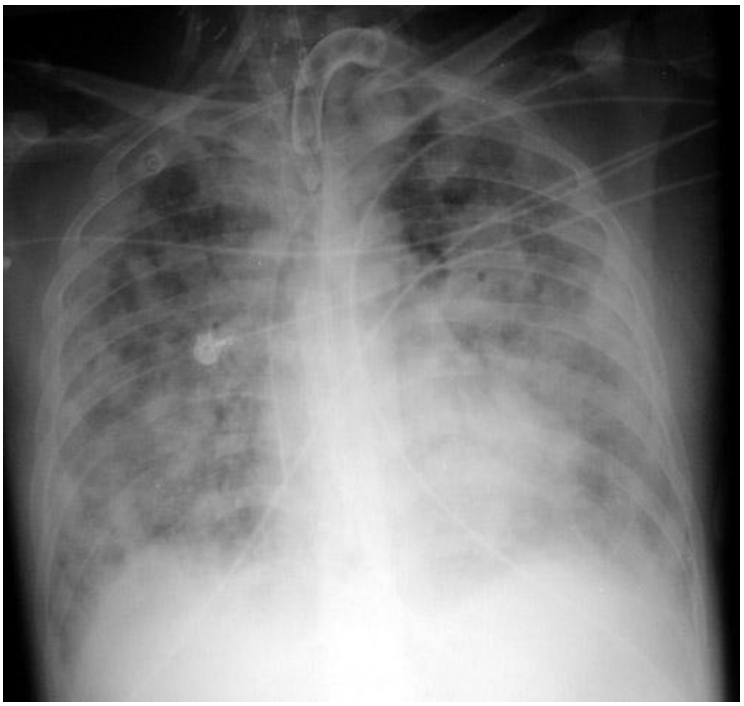

Figure 2. X-rays of both healthy (A) and ARDS patient (B).

1.2 Epidemiology and pathogenesis of ARDS

ARDS is a common syndrome, with an annual US incidence of greater than 80 per 100,000 population, and it occours especially in adults (Hudson and Steinberg, 1999). ARDS can be precipitated by either direct or indirect insult to the lung. Direct insults pertain pneumonia,

aspiration of gastric contents, pulmonary contusion, or inhalation of injurious gases. Indirect injury can occur as a result of systemic processes such as sepsis, pancreatitis, multiple trauma, or massive transfusion of blood products. Sepsis is the most frequent cause of ARDS in humans. Sepsis causes the highest mortality compared with other etiologies of ARDS (Hudson and Steinberg, 1999). Early deaths in ARDS are because of hypoxic respiratory failure and development of multiple organ failure, whereas deaths after 2 weeks are usually attributable to progressive pulmonary dysfunction as a result of exuberant fibroproliferation and the development of nosocomial infection, most notably pneumonia (Dever and Johanson, 1995;Marshall et al., 2000). In the initial phase of ARDS (referred to as the exudative phase), direct or indirect insults generally result in injury to both the capillary endothelium and the alveolar epithelium (Bachofen and Weibel, 1982;Anderson and Thielen, 1992) (Figure 3). Type I alveolar epithelial cells (AECs) comprise >95% of the alveolar surface, and are particularly susceptible to injury. As a consequence of capillary endothelial and AEC injury, there is loss of alveolar-capillary barrier function and accumulation of protein-rich edema fluid within the pulmonary interstitium and alveolus (Ware and Matthay, 2000). Denuded epithelium is replaced by the formation of proteinaceous hyaline membranes.

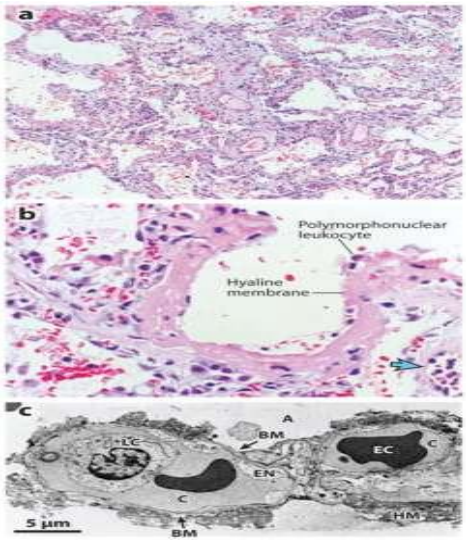

Figure 3. Anatomopathological findings in ARDS

The exudative phase of ARDS is temporally associated with influx of neutrophils within pulmonary capillaries, margination and adherence to the activated endothelium, followed by exuberant accumulation of polymorphonuclear leukocytes (neutrophils) (PMNs) in both interstitial and alveolar spaces (Steinberg et al., 1994) (Figure 3). Activated PMNs contribute to lung injury by releasing a variety of injurious molecules, including neutrophil elastase, metalloproteases, and other proteolytic enzymes, oxidants, and reactive nitrogen species (Lee and Downey, 2001;Abraham, 2003). In addition to PMNs, there is chemokine-dependent emigration of macrophages, which can amplify pulmonary injury by releasing inflammatory cytokines and apoptosis-inducing molecules (Lee and Downey, 2001) (Figure 4).

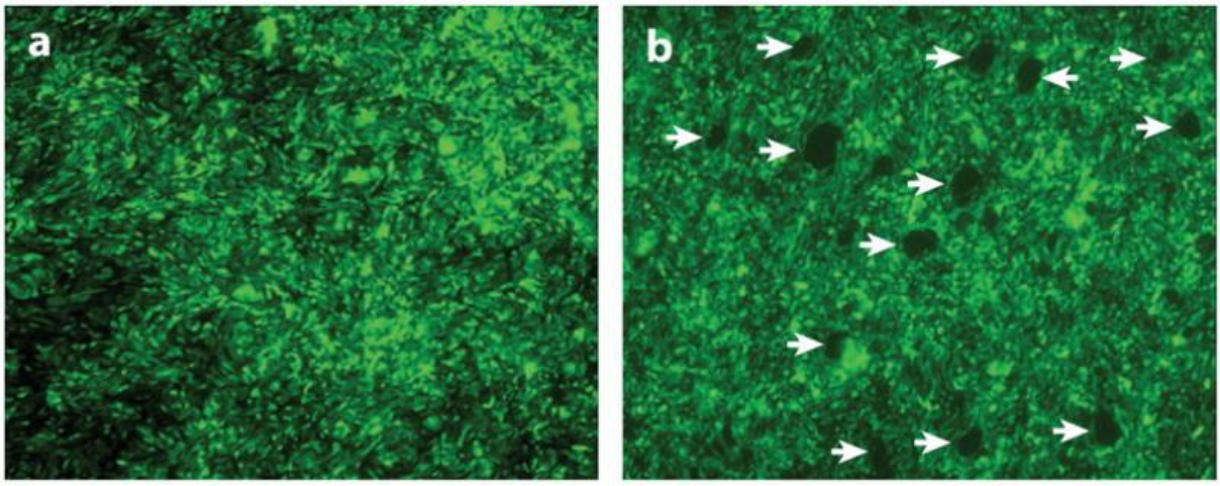

Figure 4. Alteration in the alveolar epithelium after inflammatory phenomenon.

The fibroproliferative phase of ARDS occurs early after injury (within initial 3 days) and temporally overlaps with inflammatory events that interest the exudative phase. The alveolar space becomes engorged with proliferating mesenchymal cells, such as fibroblasts, myofibroblasts, and locally generated pluripotent mesenchymal progenitor cells (Chesnutt et al., 1997;Horowitz et al., 2006) (Figure 5). Type II AECs proliferate to

replace necrotic and apoptotic type I cells, and new blood vessels form within the provisional matrix. There is also evidence of thrombogenesis and impaired fibrinolytic activity, as indicated by the accumulation of fibrin in the distal airspaces, together with microthrombi in small pulmonary vessels (Idell et al., 1989; Abraham, 2000;Prabhakaran et al., 2003). In some patients, there is pronounced deposition of matrix components, including fibronectin and replacement of type III collagen by type 1 collagen (Chesnutt et al., 1997). An exuberant fibroproliferative response in patients with ARDS is associated with a requirement for prolonged mechanical ventilation and increased mortality (Martin et al., 1995;Marshall et al., 2000).

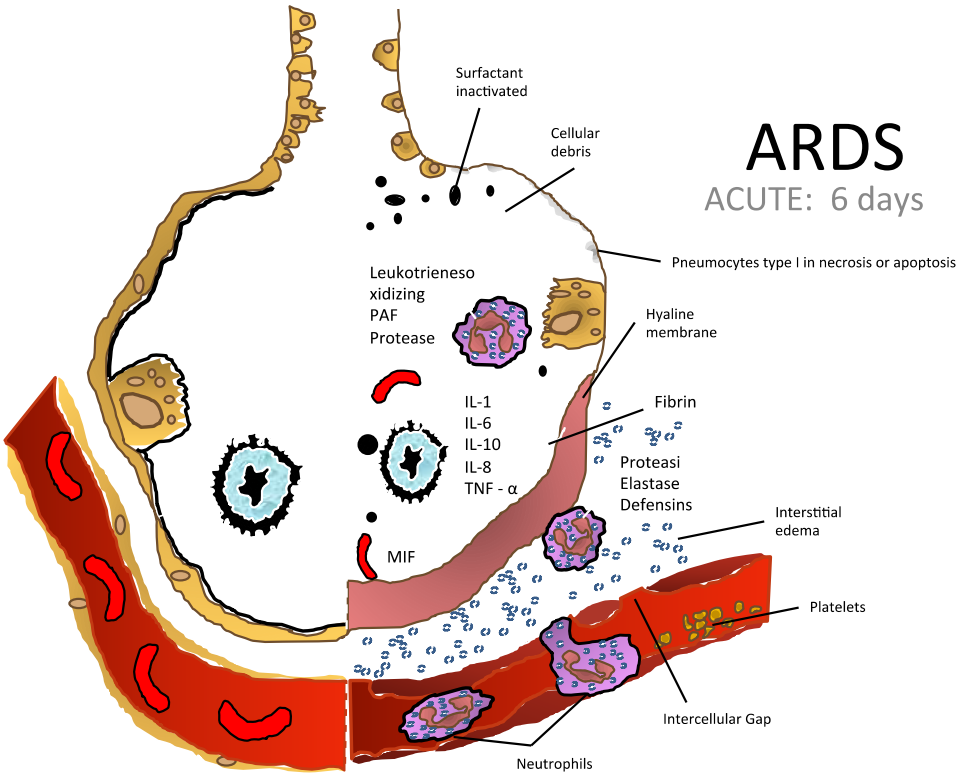

Figure 5. Pathophysiological cascade of ARDS acute phase.

CHAPTER II

ADRENOMEDULLIN

2.1 Discovery and biochemistry

Adrenomedullin (AM) was discovered in 1993 when Kitamura and her colleagues, monitoring the increased concentrations of cAMP in plates with human pheochromocytoma cells attempt, they isolated this peptide. To this molecule, known then as adrenomedullin, the authors attributed vasodilatator and hypotensive properties. The peptide is highly represented in blood and, in smaller quantities, also in urine, cerebrospinal and amniotic fluids. Human AM, consisting of 52 amino acids, has one intramolecular disulfide bond (Figure 6) (Kitamura et al., 2002).

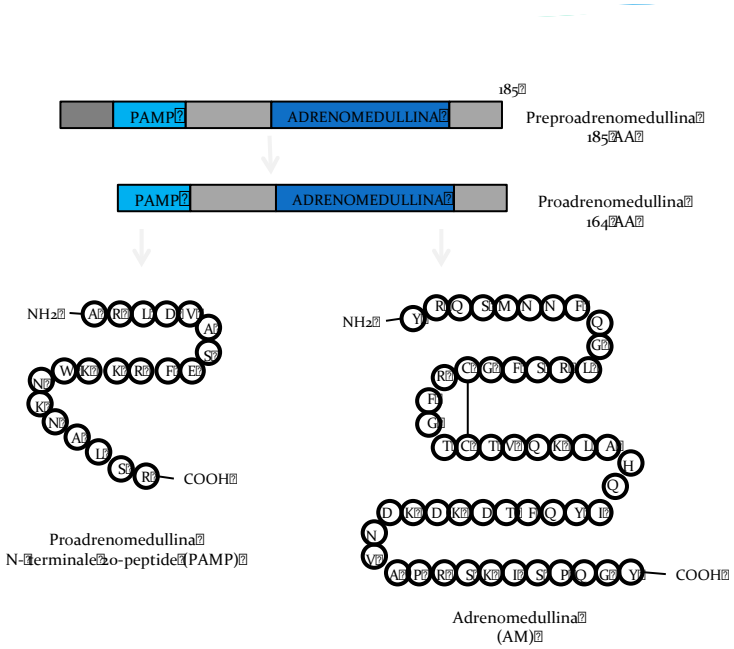

Figure 6. Adrenomedullin primary structure.

The carboxy terminal Tyr was amidated. The carboxy terminal amide structure is often observed in other biologically active peptides. AM shares structural homology with CGRP

and amylin. As shown in Figure 3a, the sequence homology of AM with human CGRP (Morris et al., 1984) and amylin (Cooper et al., 1987), is not high, although they share a six-residue ring structure formed by an intramolecular disulfide linkage and the C-terminal amide structure. It should be noted that the 14 residue amino terminal extension in AM is not found in CGRP and amylin. AM may belong to the CGRP superfamily based on its slight sequence homology and similar pharmacological activities to CGRP.

In addition to human AM, the amino acid sequence of AM has been elucidated in rat, canine, mouse, porcine, and bovine species. Porcine AM is nearly identical to the human peptide, with a single substitution (Gly for Asn) at position 40 (Kitamura et al., 1994). Rat AM has 50 amino acids, with 2 deletions and 6 substitutions compared with the human peptide (Sakata et al., 1993).

A comparison of amino acid sequences from different species is shown in Figure 6. Among these species, the ring structure and carboxy terminal amide structure, both of which are essential for biological activity (Eguchi et al., 1994), seem to be well preserved. The precursor for human AM (human preproAM)is composed of 185 amino acids in length, including the AM sequence (Kitamura et al., 1993).

The predicted sequence of proAM contains a Gly-Lys-Arg segment immediately adjacent to the C-terminal tyrosine residue of AM. GIy-X-Y, where X and Y are basic residues, can serve as signals for C-terminal amidation, a process in which the glycine residue donates an amide moiety to the free carboxylic acid group (Bradbury and Smyth, 1991). In addition to AM, proadrenomedullin (proAM) contains a unique twenty amino acid sequence followed by Gly-Lys-Arg, a typical amidation signal, in the N-terminal region. It is possible that a novel 20 residue peptide, termed “proadrenomedullin N-terminal 20 peptide (PAMP)” whose carboxy terminus is Arg-CONH2, is processed from AM precursor.

We have clarified that PAMP exists in vivo and elicits a potent hypotensive activity in anesthetized rats, as described in Proadrenomedullin N-Terminal 20 Peptide. In addition to human PAMP, the amino acid sequence of PAMP has been elucidated in rat, canine, mouse, porcine, and bovine species. Among these species, the amide structure and the amino acid sequences of PAMP in the C-terminal region seem to be well preserved, a requirement for hypotensive activity.

The genes for human and mouse AM were isolated and its structure was determined (Okazaki et al., 1996). The genomic DNA of human AM consists of 4 exons and 3 introns. The mature AM peptide is coded in the fourth exon, while PAMP is interposed by the second intron. The 5□ franking region of the AM gene contains TATA, CAAT, and CC boxes. These elements are regarded as essential to the initiation of transcription by RNA polymerase II and basal expression of the gene. In addition, there are several binding sites for activator protein-2 (AP-2) in the 5' upstream region of exon 1. Because AP-2 is assumed to mediate transcriptional activation induced by protein kinase C and cAMP, expression of the AM gene may be subject to these signal transduction pathways (Imagawa et al., 1987). Considering that AM stimulates platelet cAMP production, the multiple AP-2 sites suggest the existence of a feed- back mechanism. In intron 1, there is a consensus sequence for the cAMP-regulated enhancer (CRE) (Fink et al., 1988). This may also be involved in the putative feedback regulation of AM gene expression by cAMP. It has also been found that there are nuclear factor-kB (NF-kB) sites on the promotor of the AM gene. A study of the functional elements of the AM gene demonstrated that the nuclear factor for interleukin-6 (NF-IL-6), AP-2, and the TATA box in this region are important in the transcription regulation of the gene. These indicate that the human AM gene contains components for its functional expression, and that the expression may be subject to the

activity of protein kinase C and feedback from cAMP levels. In addition, the AM gene is found to be situated in a single locus of chromosome.

2.2 Molecular Characterization of AM Receptor

Kapas et al. (1995) cloned the cDNA for a putative AM receptor (L1) from rat lung tissue. The cDNA for L1 encodes a polypeptide of 395 residues, which possesses seven putative, alpha-helical transmembrane domains and supposed members of the G-protein-linked receptor super family.

The L1 receptor was identified as an orphan G protein-linked receptor that had been reported by two groups (Eva and Sprengel, 1993); (Harrison et al., 1993). When this putative receptor was expressed in COS-7 cells, a cAMP response to AM occurred.

But no response was found in cells stimulated with CGRP. In addition to L1, they reported that the orphan receptor RDC-1 functions as a receptor for both CGRP and AM (Kapas and Clark, 1995). However, the results concerning both L1 and RCD-1 described by Kapas et al. (1995) have not been reproduced in other laboratories.

Calcitonin receptor-like receptor (CRLR) was originally discovered as an orphan receptor that shows a 55% identity with calcitonin receptor.

This receptor expressed in COS-7 cells did not bind with members of the calcitonin/CGRP family of peptides. However, Aiyar et al. (1996) showed that human CRLR maintained its stability as it was transfected into human embryonic kidney (HEK) 293 cells exhibiting the pharmacology of CGRP1 receptor. Meanwhile, cRNA from SK-N-MC cells that expressed CGRP receptors was found to induce a novel CGRP response in Xenopus oocytes.

The protein was cloned as a receptor activity modifying protein (RAMP1) (McLatchie et al., 1998). It has 148 amino acids with a single transmembrane domain that conferred CGRP1 receptor activity to the oocytes. Co-expression of CRLR with RAMP1 was found

to create novel CGRP receptors, but expression of either protein alone was without effect. Furthermore, database searches have revealed two more RAMP proteins, RAMP2 and RAMP3, which share approximately 30% identity with RAMP1. Expression of RAMP2 or RAMP3 with CRLR leads to its expression as an AM receptor. RAMP2 and RAMP3 appear indistinguishable in terms of AM binding.

The RAMPs are required to transport CRLR to the plasma membrane. RAMP1 presents CRLR as a mature glycoprotein at the cell surface to form a CGRP receptor, whereas RAMP2 or RAMP3 transported receptors are core glycosylated and then become AM receptors. CRLR mRNA is extremely abundant in the rat lung and was shown to be associated with blood vessels by in situ hybridization studies. CRLR protein was also shown to be associated with vascular endothelial cells by immunocytochemistry.

As to the distributions of RAMPs mRNA expression in the human, rat, and mouse, RAMP1 is abundantly expressed in the brain, fat, thymus, and spleen, and RAMP2 in the lung, spleen, fat, and aorta, while RAMP3 is most abundant in the kidney and lung and is expressed ubiquitously (McLatchie et al., 1998).

Recently Kuwasako et al. (2000) clearly demonstrated that the CRLR is endocytosed together with RAMPs via clathrin-coated vesi cles, and both the internalized molecules are targeted to the degradative pathway.

Another interesting protein, the receptor component factor (RCF), was cloned on the basis of its ability to potentiate the endogenous Xenopus oocyte CGRP receptor (Luebke et al., 1996). RCF is a hydrophobic 146 amino acid protein obtained from guinea pig organ of Corti, which is a cytosolic protein with no similarity to RAMPs.

It has been recently demonstrated that RCF is essential for signal transduction of CGRP and AM, and interacts with CRLR directly within the cells (Evans et al., 2000)Namely, a

functional AM or CGRP receptor, which consists of at least three proteins: CRLR, RAMP, and RCF, couples the receptor to the intracellular signal transduction pathway (Figure 7).

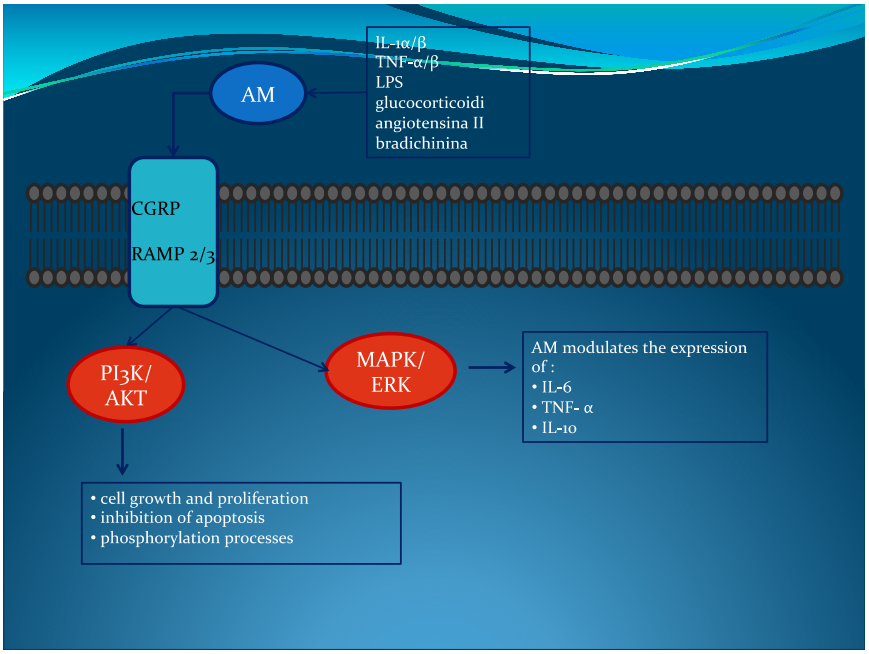

Figure 7. Adrenomedullin receptor transduction mechanisms.

CHAPTER III

AIM OF THE STUDY

The purpose of the present study was to evaluate the biological effects of adrenomedullin in both an in vitro and in vivo model of respiratory distress. In particular, we focused our attention to oxidative stress and inflammatory mechanisms.

CHAPTER IV

MATERIALS AND METHODS

4.1 Cell culture and pharmacological treatments

Human lung carcinoma A549 cells, used as a model of lung tissue cells considering the effect of LPS in ARDS, were purchased from ATCC. Cells were routinely cultured in DMEM containing 10% heat-inactivated fetal bovine serum (FBS; Lifescience Technology, Milan, Italy), 100 units/mL of penicillin, 100 μg/mL of streptomycin, and 250 ng/mL of amphotericin B (Sigma Aldrich, Milan, Italy). Cells were incubated in humidified atmosphere of 5% carbon dioxide and 95% air at 37 °C. At 80% confluency, the cells were passaged using trypsin-EDTA solution (0.05% trypsin and 0.02% EDTA). During the study cells were treated with LPS (Sigma) (0.5 μg/ml) for 1 hour. In separate set of experiments, cells were treated with Adrenomedullin (Sigma) (0.5 and 1 ng/ml) in the presence or absence of LPS.

4.2 **Cell viability evaluation cytofluorimetric analysis**

Cell viability was assessd by Muse™ Count & Viability Kit (Catalog No. MCH100102, Millipore, Milan, Italy) according to the manufacture's guidelines. Briefly, 50 μL of cell suspension containing 1 x 10^6 cells/mL were mixed with 450 μL of Count & Viability Reagent. Cells were allowed to stain for 10 minutes at room temperature and samples were read by Muse™ Cell Analyzer (Millipore).

4.3 Annexin V and dead cell evaluation by cytofluorimetric analysis

Cell apoptosis was evaluated by Muse™ Annexin V & Dead cell kit (Catalog No. MCH100105, Millipore, Milan, Italy) according to the manufacture's guidelines. Briefly, 100 μL of the Muse™ Annexin V & Dead Cell Reagent to 100 μL of cell suspension. Such

preparation was mixed thoroughly by vortexing at a medium speed for 3 to 5 seconds and samples were allowed to stain for 20 minutes at room temperature in the dark. Samples were read by Muse™ Cell Analyzer (Millipore).

4.4 Reactive Oxygen Species evaluation by cytofluorimetric analysis

Reactive oxygen species (ROS) were determined by Muse® Oxidative Stress Kit (Catalog No. MCH100111) according to the manufacture's guidelines. Briefly, 10 µL cell suspension was prepared in 1X Muse Assay Buffer and added to 190 µL of Muse® Oxidative Stress Reagent working solution. Samples were vortexed for 3 to 5 seconds and then incubated for 30 minutes at 37°C. Following incubations samples were read by Muse™ Cell Analyzer (Millipore)

4.5 Glutathione measurement

Oxidative stress in glutamate-treated cultures, in presence or absence of antioxidants, was evaluated by a colorimetric determination of GSH intracellular content. Briefly, cells were scraped off and lysed in 50 µM sodium phosphate buffer, pH 7.4. Protein concentration in cell extracts was determined by spectrophotometric analysis (Synergy HT, Biotek, Italy). Then, reduced glutathione intracellular content (GSH) was chemically determined by a colorimetric assay, as previously described.

4.6 ERK1/2 phosphorylation assessment by in-cell western

On Day 1, A549 (5000 cells/20 µl/well) were seeded in a clear bottomed, black walled 96-well plate and grown for 24 h at 37°C/5% CO_2. On Day 2, cells were treated and hen fixed in 4% PFA by adding 20 µl of 12% PFA directly to the wells for 1 h at room temperature. The wells were washed three times with PBS (50 µl/well), permeabilized with PBS/0.1%

Triton X-100 (50 µl/well, three times, 2 mins each), and blocked in LI-COR buffer (50 µl/well) for 2 hours at room temperature (or alternatively overnight at 4°C). The wells were then incubated with mouse anti-ERK1/2 or rabbit anti-phospho-ERK1/2 antibodies (1:200 for optimal signal-to-noise ratio, Cell Signalling) in LI-COR blocking buffer for 2 hours at room temperature (20 µl/well) and subsequently washed with PBS/0.1% Tween-20 (50 µl/well, three times). Infrared anti-mouse IRDye800CW and anti-rabbit IRDye700CW secondary antibodies (1: 200) in PBS/0.5% Tween-20 were then added (20 µl/well). The plates were incubated for 1 hour at room temperature, and the wells were washed with PBS/0.1% Tween-20 (three times) and incubated in PBS (50 µl/well). The plates were covered with black seals and imaged on an Odyssey infrared scanner using microplate2 settings with sensitivity of 5 in both the 700 and 800 nm wavelength channels. Data were acquired by using Odyssey software, exported and analyzed in Excel (Microsoft, Redmond, WA). Results were expressed as ratio between total ERK1/2 and phospho-ERK1/2.

4.7 RNA extraction and qRT-PCR

RNA was extracted by Trizol reagent (Invitrogen, Carlsbad, CA, USA). First strand cDNA was then synthesized with Applied Biosystem (Foster City, CA, USA) reverse transcription reagent. Quantitative real-time PCR was performed in 7900HT Fast Real-Time PCR System Applied Biosystems using the SYBR Green PCR MasterMix (Life Technologies, Milan, Italy). The specific PCR products were detected by the fluorescence of SYBR Green, the double stranded DNA binding dye. The relative mRNA expression level was calculated by the threshold cycle (Ct) value of each PCR product and normalized with that of GAPDH by using comparative $2^{-\Delta\Delta Ct}$ method.

4.8 Animals

Male Sprague Dawley rats (200 g; Charles River, Milan, Italy) were housed in a controlled environment and provided with standard rodent chow and water. Animal care was in compliance with Italian regulations on protection of animals used for experimental and other scientific purpose (D.M. 116192) as well as with the EEC regulations (O.J. of E.C. L 358/1 12/18/1986).

4.9 Experimental groups

Rats were randomized into four experimental groups:

1) LPS + vehicle group. Rats received intratracheal instillation of LPS (1 mg/kg), and the vehicle for AM (saline 0.9%w/v, (N = 10)

2) LPS + ADM (200 ng/kg) group. Identical to the LPS + vehicle group but they were also administered AM intratracheally (200 ng/kg) (N = 10)

3) LPS + ADM (400 ng/kg) group. Identical to the LPS + vehicle group but they were also administered AM intratracheally (400 ng/kg) (N = 10)

4) Sham + vehicle group. Identical to the LPS + vehicle group but animals received intratracheal

instillation of saline (0.9% w/v), instead of LPS, (N = 10).

5) Sham + ADM group (200 ng/kg). Identical to the LPS + AM group but animals received intratracheal instillation of saline (0.9% w/v) instead of LPS, and were treated with AM (200 ng/kg) intratracheally (N = 10).

6) Sham + ADM group (400 ng/kg). Identical to the LPS + AM group but animals received intratracheal instillation of saline (0.9% w/v) instead of LPS, and were treated with AM (400 ng/kg) intratracheally (N = 10).

Rats were killed 24h following LPS treatment in order to evaluate the early mechanisms involved in acute lung injury.

4.10 Induction of lung injury by LPS

Rats received a single intratracheal instillation of saline (0.9% w/v) or saline containing LPS (1 mg/kg body weight) at end-expiration in a volume of 100 μL and the liquid was followed immediately by 300 μL of air, to ensure delivery to the distal airways.

4.11 Measurement of fluid content in lung

The wet lung weight was measured by careful excision of the lung from other adjacent extraneous tissues. The lung was exposed for 48 h at 180°C and the dry weight was measured. Water content was calculated by subtracting dry weight from wet weight.

4.12 Histological examination

Excised lung were taken 24h after LPS injection were fixed for 1 week in 10% (w/v) PBS-buffered formaldehyde solution at room temperature, dehydrated, using graded ethanol and embedded in Paraplast (Sherwood Medical, Mahwah, NJ, USA). The sections were prepared and stained by hematoxylin and eosin and observed using light microscopy

4.13 Citokynes Proteome Profiler Array

To conduct a Proteome Profiler array experiment, lungs were rinsed twice with PBS, and Nonidet P-40 lysis buffer was added. Tissue homogenates were gently rocked for 30 min at 4 °C and then centrifuged at 14,000_g for 5 min (4 °C), and the supernatants were frozen at -80 °C. A total of 250 micrograms of protein was used for each array. To prevent

unspecific protein binding, arrays were blocked using 2% bovine serum albumin in PBS for 1 h at room temperature. Subsequently tissue homogenates were diluted with PBS containing 2% bovine serum albumin, and the arrays were incubated with the diluted samples overnight at 4 °C. The arrays were then washed three times for 10 min with a wash buffer as specified by the manufacturer. After another washing step both types of arrays were processed using a luminol-based reagent, which is used in combination with LiCor secondary antibodies (Carlo Erba, Milan, Italy). Subsequently, arrays were analyzex with LiCor array scanner.

4.14 Statistical Analysis

Statistics were aided by Graph Pad Prism. All results were expressed as mean ± standard error of mean (S.E.M.). P values less than 0.05 were considered significant. Biochemical data were analyzed by one-way ANOVA with Bonferroni Post-Hoc analysis. Concentration-response curve from isolated pulmonary arteries were compared by two-way ANOVA.

CHAPTER V

RESULTS

5.1 Cell Viability

Our data suggest that LPS treatment for 1 hour resulted in a signficant ($p<0.05$) reduction of cell viability (Figure 8). Interestingly, ADM treatment resulted in a dose dependent effect on cell viability. In fact, we observed a significant ($p<0.05$) increase of cell viability with a dose of 0,5 ng/ml of ADM whereas 1 ng/ml resulted in a significant ($p<0.05$) worsening of viability.

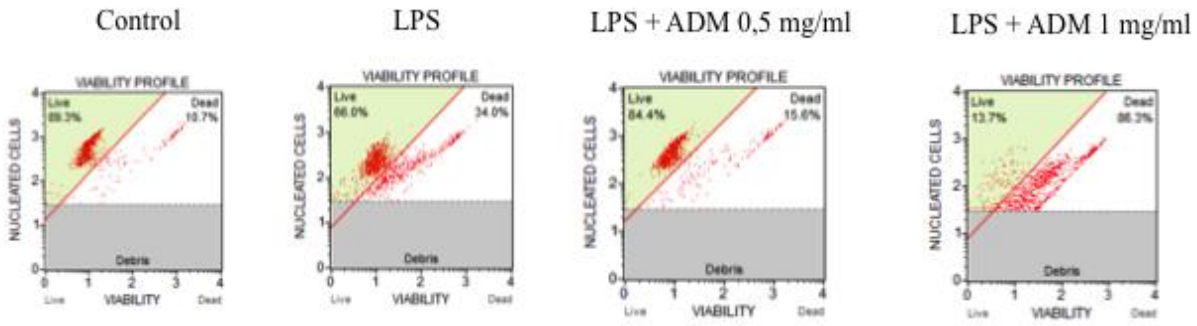

Figure 8. Cytofluorimetric analysis of cell viability. Experiments were performed in triplicate. Picture is representative of a single experiment.

5.2 Apoptosis evaluation by cytofluorimetric Annexin V expression

LPS treatment resulted in a significant ($P<0.05$) increase of apoptotic cell death compared to untreated cultured cells (Figure 9). Consistently with cell viability results, we showed a dose dependent effect of ADM on cell apoptosis. In fact, we observed a significant ($p<0.05$) decrease of apoptosis with a dose of 0,5 ng/ml of ADM whereas 1 ng/ml resulted in a significant ($p<0.05$) worsening of apoptotic cell death.

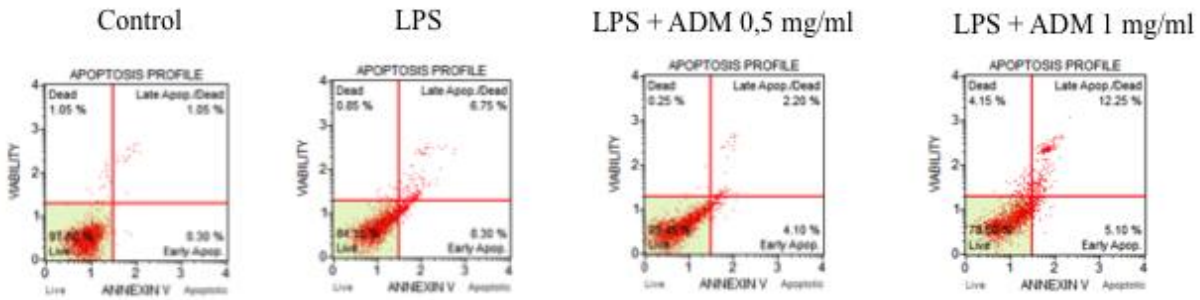

Figure 9. Cytofluorimetric analysis of cell apoptosis by Annexin V assay. Experiments were performed in triplicate. Picture is representative of a single experiment.

5.3 Reactive Oxygen Species formation

Figure 10 shows that LPS treatment resulted in a significant increase in ROS formation. ADM (0,5 ng/ml) resulted in a significant decrease of ROS formation whereas ADM (1 ng/ml) exacerbated ROS formation when compared to untreated cell cultures.

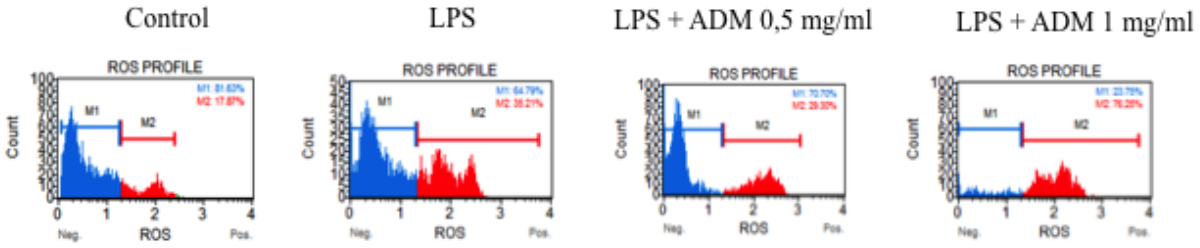

Figure 10. Cytofluorimetric analysis of intracellular ROS content. Experiments were performed in triplicate. Picture is representative of a single experiment.

5.4 Reduced glutathione content measurement

In order to further demonstrate the protective and antioxidant properties of ADM, we also determined the intracellular content of reduced GSH. Our data suggest that LPS treatment results in a significant ($p<0.05$) decrease of GSH compared to untreated cells (Figure 11). ADM (0,5 ng/ml) restored GSH content in LPS treated cells. By contrast, ADM (1 ng/ml) significanttly ($p<0.05$) reduced GSH content compared to LPS treatment alone.

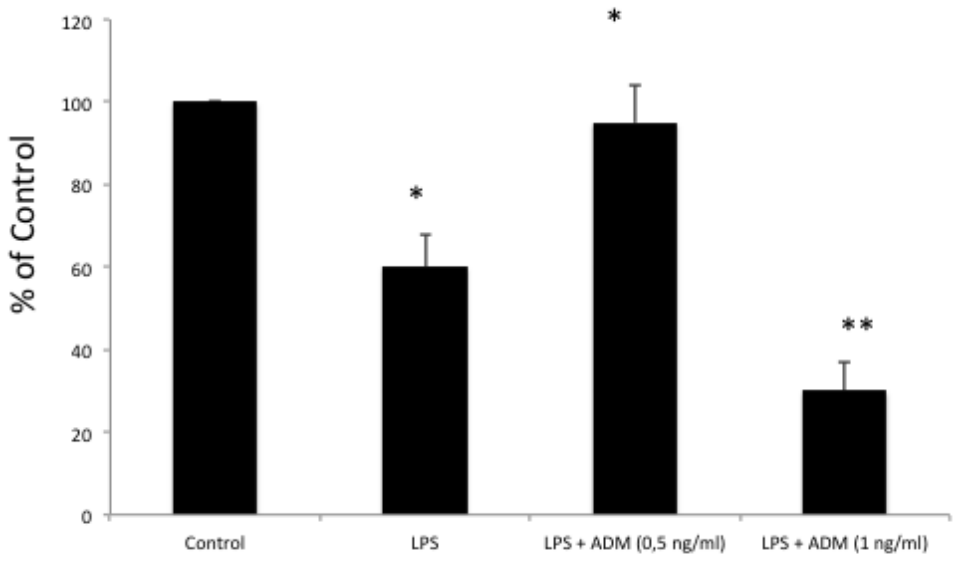

Figure 11. Spectrophotometric analysis of intracellular GSH content. Experiments were performed in triplicate and results are presented as percentage of the control. (*P<0.05 when compared to control; **P<0.05 when compared to LPS).

5.5 ERK1/2 phosphorylation assessment by in-cell western

In order to further evaluate the molecular mechanism underlying ADM treatment we evaluated the phosphorylation of ERK-1/2, which is known to be activated also following LPS treatment. This set of experiment showed a significant increase of ERK1/2 phosphorylation following LPS treatment (Figure 6). Interestingly, ADM (0,5 ng/ml) treatment at was able to prevent ERK1/2 activation. No significant effect was observed on ERK-1/2 phosphorylation following ADM (1 ng/ml) when compared to LPS treatment alone.

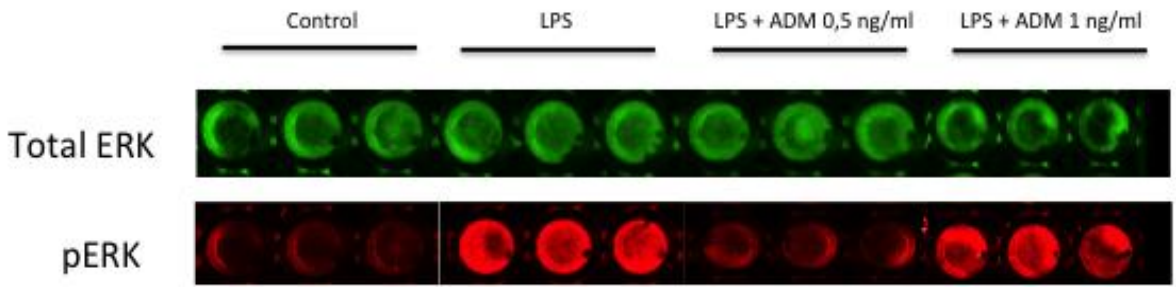

Figure 12. In cell western for evaluation of pERK. Experiments were performed in triplicate on a 96 well plate. Three independent wells are represented in the picture for each treatment. Green fluorescent represents total ERK whereas red fluorescence indicated ERK phosphorylation.

5.6 Inflammatory mediators gene expression

Our data showed that LPS treatments results in a significant activation of the inflammatory response as measured by the increased gn of well established inflammatory gene such as IL-6 (Figure 13). TNF-alpha, IL-8, IL-1 beta and MCP-1. ADM (0,5 ng/ml) resulted in a significant reduction of the inflammatory response when compared to LPS treated cells. By contrast, ADM (1 ng/ml) exacerbated the inflammatory response when compared to LPS treated cells or untreated cell cultures.

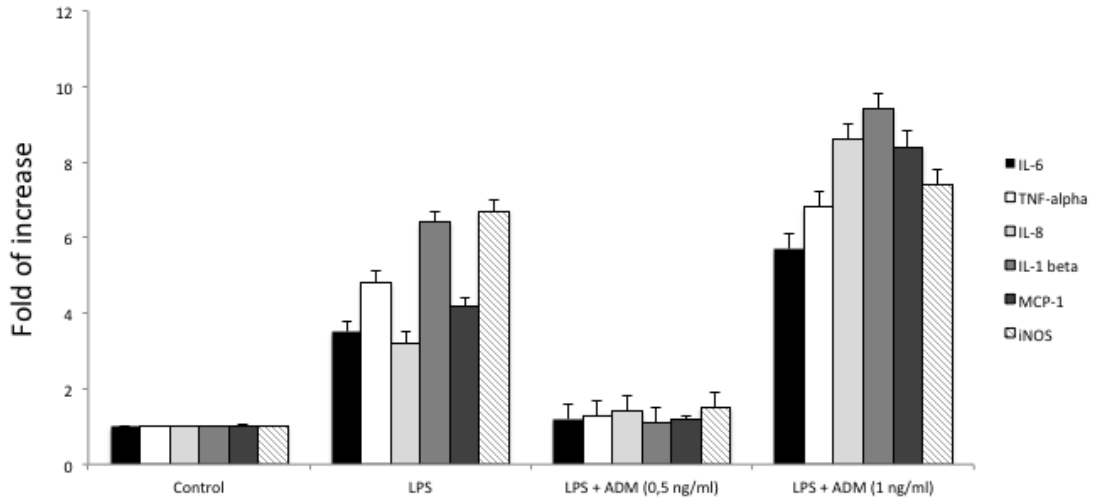

Figure 13. Real time PCR evaluating various inflammatory mediators gene expression. Results are expressed as fold of increase compared to relative controls.

5.7 Effects of AM on LPS-induced lung injury and fluid content

Twenty-four hours after LPS administration the pulmonary lesions observed in rats consisted of multifocal areas of severe inflammation and parenchymal lesions (Figure 14A). ADM (200 ng/kg) resulted in a significant reduction od lung injury whereas ADM (400 ng/kg) had no significant effect on parenchyma injury. Similarly, ADM (200 ng/kg) resulted in a significant reduction of lung edema as measured by wet/dry weight ratio when compared to LPS treated animals (Figure 14B).

A

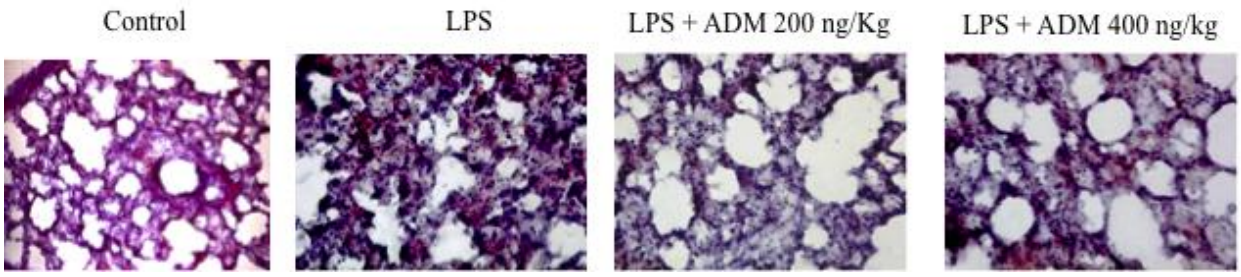

B

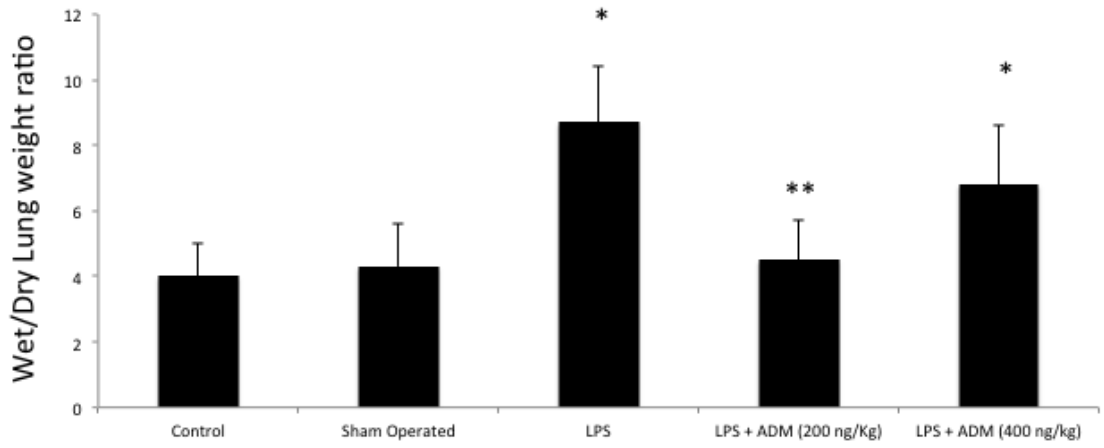

Figure 14. (A) Histopathological findings (H&E staining) of rat lungs following intratracheal injection of LPS in the presence or absence of adrenomedullin treatment at various concentrations. Sham operated animals were referred as controls. (B) Wet/Dry lung weight ratio determination for the assessment of lung edema formation. (*$p<0.05$ when compared to control; **$p<0.05$ when compared to LPS).

5.8 Citokynes Proteome Profiler Array

In order to further confirm the in vivo protective effects of ADM, on the basis of the in vitro results we performed a citokyne proteome profiler array. These set of experimets confirmed that the in vitro inflammatory mediators are also upregulate at protein levels in the animal model of acute lung injury (Figure 15). Furthermore, we also showed that ADM (200 ng/Kg) exhibithed anti-inflammatory properties as shown by reduction of IL-6. TNF-alpha, IL-8, IL-1 beta and MCP-1. No significant effects were observed for ADM (400 ng/Kg) when compared to LPS treated animals.

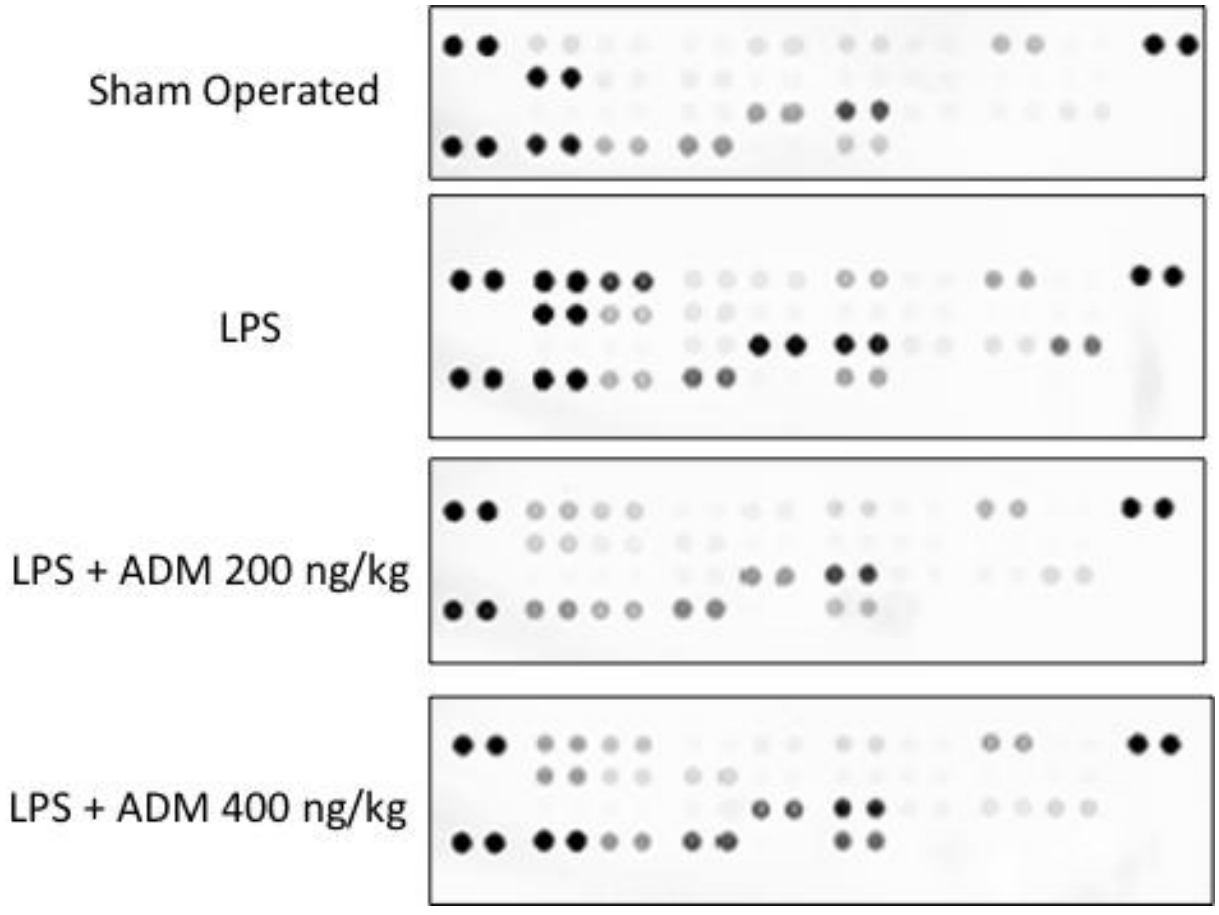

Figure 15. Citokynes Proteome Profiler Array for the evaluation of inflammatory cytokines production. Each cytokyne is spotted in duplicate on each membrane and intensity was determined by image J software.

CHAPTER VI

DISCUSSION

This study examined the beneficial effect of ADM on LPS-induced pulmonary injury; in particular, our results indicate that ADM has strong antioxidant, anti-inflammatory and antiapoptotic properties both in vitro and in vivo in a dose dependent manner. ADM can play a master role in orchestrating differential regulation among tissues during inflammation because of its capacity to bind to multiple classes of receptors and elicit different tissue responses in specific tissue sites. In essence, ADM is both a hormone and a cytokine. It can simultaneously regulate aspects of regional blood flow, immunological recruitment, and preferential nutrient use by tissues during the inflammatory response. Many of the responses of body tissues to an inflammatory insult are triggered and modulated by cytokines. Most relevant to the topic at hand is the tight relationship between proinflammatory cytokines, like TNF-a and IL-1b , and ADM during the onset of systemic as well as localized tissue inflammatory response. In our LPS model, it has been shown that

the cytokine network is capable of modulating the different phases of lung injury pathogenesis in a dose dependent manner. Among the several cytokines and chemokines that have been implicated in the pathogenesis of lung injury, particular relevance has been given to IL-1 and TNF-a . Recent studies suggest that ADM plays a role in the complex network of pulmonary cytokines. In vitro data showed that ADM inhibits cytokine-induced neutrophil chemoattractant secretion from lipopolysaccharide-stimulated rat alveolar macrophages, and suppress TNF-a production in IL-1b stimulated Swiss 3T3 cells. An in vivo study demonstrates a significant suppression of pulmonary TGF-b 1 and IL-1b mRNA expression by aerosolized ADM [23]. In the present study, we confirm that the model of lung injury used leads to a substantial increase in the levels of TNF-a and IL-1 in

the lung after LPS administration and we report by first time that the production of the pro-inflammatory cytokines are significantly attenuated by the treatment with ADM with low dose. There is compelling evidence that endogenous NO plays a key role in physiological regulation of airway functions and is implicated in airway disease. In an inflammatory micro environment NO, and related compounds, are produced by a wide variety of residential and inflammatory cells in the respiratory system [27]. This reaction is catalyzed by iNOS in macrophages and epithelial, endothelial, and vascular smooth-muscle cells. This isoform is regulated at a pre-translational level and can be induced by proinflammatory cytokines, such as TNF-**a** , and IL-1**b** .

Conclusions

These data support the hypothesis that ADM is an inhibitor of LPS-induced lung injury and this protective effect is observed also by a significant reduction of the oedema formation, tissue damage and reduced content of inflammatory mediators. In conclusion, we hypothesize that the antiinflammatory properties of ADM may be related to its ability to decrease the production and expression of proinflammatory cytokines, as our work has demonstrated. This property leads us to imagine the existence of an intricate interaction between ADM and cytokines, leading to a modulation of inflammatory process associated with lung injury.

Acknowledgment

I wish to express my deep gratitude to Prof. Sabrina David and Giovanni Li Volti for supporting me during the project of my PhD thesis with their guidance and insightful knowledge. Their constant presence, gentleness and advice have been greatly appreciated.

I would like to thank my loved ones, who have willingly shared their precious time with me and have supported me throughout the entire process.

REFERENCES

Abraham, E. (2000). Coagulation abnormalities in acute lung injury and sepsis. *Am J Respir Cell Mol Biol* 22**,** 401-404.

Abraham, E. (2003). Neutrophils and acute lung injury. *Crit Care Med* 31**,** S195-199.

Anderson, W.R., and Thielen, K. (1992). Correlative study of adult respiratory distress syndrome by light, scanning, and transmission electron microscopy. *Ultrastruct Pathol* 16**,** 615-628.

Ashbaugh, D.G., Bigelow, D.B., Petty, T.L., and Levine, B.E. (1967). Acute respiratory distress in adults. *Lancet* 2**,** 319-323.

Bachofen, M., and Weibel, E.R. (1982). Structural alterations of lung parenchyma in the adult respiratory distress syndrome. *Clin Chest Med* 3**,** 35-56.

Chesnutt, A.N., Matthay, M.A., Tibayan, F.A., and Clark, J.G. (1997). Early detection of type III procollagen peptide in acute lung injury. Pathogenetic and prognostic significance. *Am J Respir Crit Care Med* 156**,** 840-845.

Cooper, G.J., Willis, A.C., Clark, A., Turner, R.C., Sim, R.B., and Reid, K.B. (1987). Purification and characterization of a peptide from amyloid-rich pancreases of type 2 diabetic patients. *Proc Natl Acad Sci U S A* 84**,** 8628-8632.

Dever, L.L., and Johanson, W.G., Jr. (1995). Pneumonia complicating adult respiratory distress syndrome. *Clin Chest Med* 16**,** 147-153.

Eguchi, S., Hirata, Y., Kano, H., Sato, K., Watanabe, Y., Watanabe, T.X., Nakajima, K., Sakakibara, S., and Marumo, F. (1994). Specific receptors for adrenomedullin in cultured rat vascular smooth muscle cells. *FEBS Lett* 340**,** 226-230.

Eva, C., and Sprengel, R. (1993). A novel putative G protein-coupled receptor highly expressed in lung and testis. *DNA Cell Biol* 12**,** 393-399.

Evans, B.N., Rosenblatt, M.I., Mnayer, L.O., Oliver, K.R., and Dickerson, I.M. (2000). CGRP-RCP, a novel protein required for signal transduction at calcitonin gene-related peptide and adrenomedullin receptors. *J Biol Chem* 275**,** 31438-31443.

Fink, J.S., Verhave, M., Kasper, S., Tsukada, T., Mandel, G., and Goodman, R.H. (1988). The CGTCA sequence motif is essential for biological activity of the vasoactive intestinal peptide gene cAMP-regulated enhancer. *Proc Natl Acad Sci U S A* 85**,** 6662-6666.

Harrison, J.K., Barber, C.M., and Lynch, K.R. (1993). Molecular cloning of a novel rat G-protein-coupled receptor gene expressed prominently in lung, adrenal, and liver. *FEBS Lett* 318**,** 17-22.

Horowitz, J.C., Cui, Z., Moore, T.A., Meier, T.R., Reddy, R.C., Toews, G.B., Standiford, T.J., and Thannickal, V.J. (2006). Constitutive activation of prosurvival signaling in alveolar mesenchymal cells isolated from patients with nonresolving acute respiratory distress syndrome. *Am J Physiol Lung Cell Mol Physiol* 290**,** L415-425.

Hudson, L.D., and Steinberg, K.P. (1999). Epidemiology of acute lung injury and ARDS. *Chest* 116**,** 74S-82S.

Idell, S., James, K.K., Levin, E.G., Schwartz, B.S., Manchanda, N., Maunder, R.J., Martin, T.R., Mclarty, J., and Fair, D.S. (1989). Local abnormalities in coagulation and fibrinolytic pathways predispose to alveolar fibrin deposition in the adult respiratory distress syndrome. *J Clin Invest* 84**,** 695-705.

Imagawa, M., Chiu, R., and Karin, M. (1987). Transcription factor AP-2 mediates induction by two different signal-transduction pathways: protein kinase C and cAMP. *Cell* 51**,** 251-260.

Kapas, S., and Clark, A.J. (1995). Identification of an orphan receptor gene as a type 1 calcitonin gene-related peptide receptor. *Biochem Biophys Res Commun* 217**,** 832-838.

Kitamura, K., Kangawa, K., and Eto, T. (2002). Adrenomedullin and PAMP: discovery, structures, and cardiovascular functions. *Microsc Res Tech* 57**,** 3-13.

Kitamura, K., Kangawa, K., Kojima, M., Ichiki, Y., Matsuo, H., and Eto, T. (1994). Complete amino acid sequence of porcine adrenomedullin and cloning of cDNA encoding its precursor. *FEBS Lett* 338**,** 306-310.

Kitamura, K., Sakata, J., Kangawa, K., Kojima, M., Matsuo, H., and Eto, T. (1993). Cloning and characterization of cDNA encoding a precursor for human adrenomedullin. *Biochem Biophys Res Commun* 194**,** 720-725.

Lee, W.L., and Downey, G.P. (2001). Neutrophil activation and acute lung injury. *Curr Opin Crit Care* 7**,** 1-7.

Luebke, A.E., Dahl, G.P., Roos, B.A., and Dickerson, I.M. (1996). Identification of a protein that confers calcitonin gene-related peptide responsiveness to oocytes by using a cystic fibrosis transmembrane conductance regulator assay. *Proc Natl Acad Sci U S A* 93**,** 3455-3460.

Marshall, R.P., Bellingan, G., Webb, S., Puddicombe, A., Goldsack, N., Mcanulty, R.J., and Laurent, G.J. (2000). Fibroproliferation occurs early in the acute respiratory distress syndrome and impacts on outcome. *Am J Respir Crit Care Med* 162**,** 1783-1788.

Martin, C., Papazian, L., Payan, M.J., Saux, P., and Gouin, F. (1995). Pulmonary fibrosis correlates with outcome in adult respiratory distress syndrome. A study in mechanically ventilated patients. *Chest* 107**,** 196-200.

Mclatchie, L.M., Fraser, N.J., Main, M.J., Wise, A., Brown, J., Thompson, N., Solari, R., Lee, M.G., and Foord, S.M. (1998). RAMPs regulate the transport and ligand specificity of the calcitonin-receptor-like receptor. *Nature* 393**,** 333-339.

Okazaki, T., Ogawa, Y., Tamura, N., Mori, K., Isse, N., Aoki, T., Rochelle, J.M., Taketo, M.M., Seldin, M.F., and Nakao, K. (1996). Genomic organization, expression, and chromosomal mapping of the mouse adrenomedullin gene. *Genomics* 37**,** 395-399.

Prabhakaran, P., Ware, L.B., White, K.E., Cross, M.T., Matthay, M.A., and Olman, M.A. (2003). Elevated levels of plasminogen activator inhibitor-1 in pulmonary edema fluid are associated with mortality in acute lung injury. *Am J Physiol Lung Cell Mol Physiol* 285**,** L20-28.

Sakata, J., Shimokubo, T., Kitamura, K., Nakamura, S., Kangawa, K., Matsuo, H., and Eto, T. (1993). Molecular cloning and biological activities of rat adrenomedullin, a hypotensive peptide. *Biochem Biophys Res Commun* 195**,** 921-927.

Steinberg, K.P., Milberg, J.A., Martin, T.R., Maunder, R.J., Cockrill, B.A., and Hudson, L.D. (1994). Evolution of bronchoalveolar cell populations in the adult respiratory distress syndrome. *Am J Respir Crit Care Med* 150**,** 113-122.

Ware, L.B., and Matthay, M.A. (2000). The acute respiratory distress syndrome. *N Engl J Med* 342**,** 1334-1349.